Available online at www.sciencedirect.com
SCIENCE DIRECT®

International Journal of Engineering Science 43 (2005) 1377–1387

International Journal of Engineering Science

www.elsevier.com/locate/ijengsci

Hydrodynamic modelling of a direct drive wave energy converter

M. Eriksson *, J. Isberg, M. Leijon

Department of Engineering Science, Swedish Centre for Renewable Electric Energy Conversion, Uppsala University, Box 534, SE-75121 Uppsala, Sweden

Received 4 December 2004; received in revised form 16 May 2005; accepted 25 May 2005

Abstract

In this article we present numerical studies of waves interacting with a cylindrical point absorber that is directly driving a seabed based linear generator. For waves useful for power conversion, the wave/point absorber interaction can be modelled, using potential theory assuming an inviscid irrotational incompressible fluid. The generator is modelled as a viscous damper. This paper pays special attention to the case when the converter is in resonance with the wave. The power capture capability of the system has been studied both for a harmonic wave and for real ocean waves.

Keywords: Wave energy; Resonance; Linear generator; Ocean waves; Potential wave theory; Point absorber

1. Introduction

Wave power devices are traditionally using conventional high speed rotating generators for energy conversion. This requires a system that converts the slow linear/rotation motion of the wave energy absorber to a high speed rotating motion. Hydraulic systems or turbines are used for this purpose. Such a solution gives a complex system with many moving parts. An alternative to the hydraulic systems are direct drive energy converters [1] with a linear generator. Although linear generators are fairly new for wave energy applications [2], the first electric linear motor was patented more than 100 years ago in the USA [3]. The advantage with these generators is the reduction in complexity and fewer movable parts, which in turn leads to less maintenance [4]. The drawback is a more complicated transmission to grid, since the voltage will vary in both frequency and amplitude.

In this paper we consider a concept for electric energy extraction from water waves based on a linear generator located at the sea floor [5,6]. The alternator of the generator is connected by a rope to a buoy, located on the sea surface. The alternator is also connected by a spring to the mooring system (see Fig. 1). The hydrodynamical action of water waves force the buoy and thereby the alternator to move with a vertical motion.

* Corresponding author. Tel.: +46 18 471 5818; fax: +46 18 471 5810.
E-mail address: Mikael.Eriksson@angstrom.uu.se (M. Eriksson).

0020-7225/$ - see front matter
doi:10.1016/j.ijengsci.2005.05.014

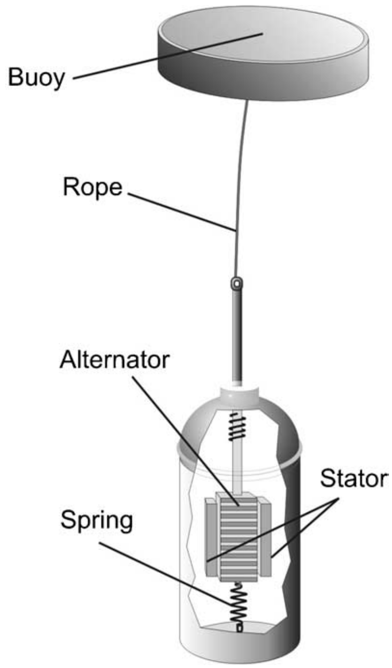

Fig. 1. Schematic figure of the converter.

The moving alternator, which is equipped with permanent magnets, induces currents in the stator windings according to Faraday's law of induction. In this way a substantial part of the energy in the waves can be converted into electric energy. In this article we present a study of the hydrodynamical interaction of harmonic and realistic waves with the buoy-generator system, using linear potential theory.

In order to calculate the excitation force and hydrodynamic parameters for the partially submerged buoy we assume, for simplicity, the buoy to be a cylinder moving in heave. For this purpose we make use of analytical expressions derived by Bhatta and Rahman [7]. These expressions are derived using variable separation and eigenfunction expansion of the velocity potential in cylindrical coordinates. Similar methodology has been used before in various ways by Miles and Gilbert [8], Garret [9], Yeung [10], Sabuncu and Calisal [11] and others.

This paper is intended to give an estimate of different parameters, such as buoy radius spring constant and generator damping coefficient in order to obtain high power capture ratio. In particular we are interested to investigate the influence of resonance on the power extraction capacity of the whole system. The converter has been simulated in a harmonic wave and in two wave climates: one measured and one with a JONSWAP spectrum [12,13].

2. Modelling

2.1. Equation of motion

As the point absorber we consider a circular cylinder with radius a, with the axis oriented in the vertical (z) direction. The cylinder is partially submerged, with draft d, in water of finite depth h. A surface wave is incident on the cylinder and the wave–buoy interaction gives rise to forces acting on the cylinder and to a scattered wave. The incident wave can be of arbitrary shape but is assumed to be plane parallel.

A rigid floating body has six degrees of freedom. We will restrict the discussion to vertical (heave) motion only. This is reasonable since our interest lies in modelling wave power converters with a point absorber tethered directly above a generator located at the seafloor. By assuming that the length of the tether is much larger than the buoy motion (in any direction) only the heave motion will appreciably affect the alternator motion and the power extraction. Furthermore, in the linear theory the different force contributions are decoupled and can be considered separately.

The vertical acceleration, $\ddot{z}$, of buoy and alternator from their equilibrium positions is related to the forces acting on the bodies by

$$m\ddot{z} = F_{\mathrm{mech}} + F_{\mathrm{gen}} + F_{\mathrm{cyl}}, \tag{1}$$

where m is the total mass of buoy and alternator, F_{mech} is mechanical force (i.e. gravity), F_{gen} is the counteracting generator force, and F_{cyl} are hydrodynamic forces acting on the cylinder. The tether connecting the point absorber and alternator is modelled as a rigid bar. This is reasonable assuming the constant downward forces acting on the alternator, such as the gravity and static spring force, are large enough to keep the tether stretched.

The mechanical force acting on the system is the spring force, which is proportional to the alternator displacement,

$$F_{\mathrm{mech}} = -k_{\mathrm{s}}z, \tag{2}$$

where k_{s} is the spring constant and z is the vertical displacement from the equilibrium position. In reality the spring acts as energy storage. When the buoy is lifted by a wave, some energy is converted to electricity in the generator and some is stored in the spring, which will be converted to electricity in the downward motion.

The generator is modelled as a viscous damper; this model presumes that the alternator length is long enough to stay inside the stator for the whole stroke. This simple model of the generator agrees well for higher velocities, for low velocities there will be some non-linear effects. The calculation of the damping coefficient for a specific generator is made using a FEM based generator simulation tool [14]. The induced force in the generator counteracts the motion and it is therefore proportional to the velocity. The generator force is thus:

$$F_{\mathrm{generator}} = -\gamma\dot{z}, \tag{3}$$

where γ is the damping coefficient. In reality, the size of γ is dependent on the amount of power the generator delivers to the grid. It is possible to adjust this when the generator is in operation using power electronics. A generator producing 10 kW for an alternator velocity of 0.7 m/s has a damping coefficient $\gamma \approx 20$ kN s/m.

The hydrodynamic forces acting on the cylinder can be derived from the two basic hydrodynamic equations: the continuity and Navier–Stokes equation. By assuming an irrational, incompressible, and ideal fluid and linearizing, the Navier–Stokes equation is simplified to the Laplace equation:

$$\nabla^2\phi = 0, \tag{4}$$

where ϕ is the velocity potential in the fluid. Thus the problem can be described by linear potential theory. The assumptions above make the wave theory valid only for reasonably small waves, which are actually usable for power extraction. The force acting on the buoy is calculated from the velocity potential, from Bernoulli's law [15].

The linearity of the Laplace equation allows the velocity potential to be decomposed into two potentials, $\phi = \phi_{\mathrm{r}} + \phi_{\mathrm{e}}$, where ϕ_{r} is a solution to the radiation problem, and ϕ_{e} a solution to the excitation problem. The radiation problem is calculated for an oscillating body in calm water and the excitation problem concerns the scattering of an incident wave on a fixed body. Because the Laplace equation is separable in cylindrical coordinates it is possible to find solutions to both the radiation and excitation problems by separation of variables, i.e. the solutions can be written as

$$\phi(r,\theta,z) = \sum_m Z(z)R(r)\cos(m\theta).$$

Solutions of this form can be found in [7].

The hydrodynamic force acting on the cylinder can be divided into three force contributions,

$$F_{\mathrm{cyl}} = F_{\mathrm{e}} + F_{\mathrm{r}} + F_{\mathrm{h}}, \tag{5}$$

where F_{e} is the force associated with the excitation problem F_{r} the force associated with the radiation problem and F_{h} is the buoyancy stiffness.

The buoyancy stiffness is proportional to the vertical elevation for a cylinder and is given by,

$$F_h = -\rho g \pi a^2 z, \tag{6}$$

where ρ is the density of water, and z the elevation.

The excitation velocity potential ϕ_e can be decomposed into two contributions: the undisturbed incident wave velocity potential and the diffracted wave velocity potential. The force associated with the former contribution is the Froude–Krylov force. For a cylinder radius which is small compared to the wavelength, the diffracted velocity potential can be neglected and then the excitation force equals the Froude–Krylov force. We cannot assume that the cylinder is small, so we need to use expressions for the full excitation force F_e.

The solution of the radiation velocity potential is done in the same way as for the excitation velocity potential. This case is somewhat simpler due to full axisymmetry. For a detailed derivation of the hydrodynamic parameters for a cylindrical buoy, see [7].

In the frequency domain the relation between the excitation force (F_e) and the amplitude of the incoming wave (G) is given by a transfer function $\hat{f}_e$,

$$\widehat{F}_e(\omega) = \hat{f}_e(\omega)\widehat{G}(\omega). \tag{7}$$

Here a caret ($\hat{}$) denotes the Fourier transform of a function. The absolute value and the argument of the transfer function $\hat{f}_e$ for a cylinder with radius a, and draft $b = 1.5$ m in water of depth $h = 23$ m is shown in Figs. 2 and 3 respectively. Furthermore, a draft $b = 1.5$ m gives an unbalance between the total weight (buoy and piston) and the buoyancy force, this will be compensated with a mooring and a concrete foundation. An unbalance is necessary to get a pre-tension in the springs and to keep the tether stretched (see Fig. 1).

Similarly, the radiation force F_r is given by a transfer function from the alternator/buoy velocity in the frequency domain,

$$\widehat{F}_r(\omega) = -(R + i\omega m_a)\hat{\dot{z}}. \tag{8}$$

Here R is the radiation resistance, and m_a, is the added mass. The hydrodynamical parameters are shown in Figs. 4 and 5. The calculations of the hydrodynamic coefficients have been verified for several specific cases and compared with numerical calculations made by Falnes [15] as well as with results from Wu et al. [16] and Drobyshevski [17]. The expressions contain infinite sums with fast convergence.

Taking the Fourier transform of Eq. (1) with Eqs. (2), (3), and (5)–(8) inserted, gives:

$$(-\omega^2(m_a + m) + i\omega(\gamma + R) + \rho g \pi a^2 + k_s)\hat{z} = \hat{f}_e\widehat{G}. \tag{9}$$

This expression can be written as

$$\hat{z} = \widehat{H}(\omega)\widehat{G}(\omega), \tag{10}$$

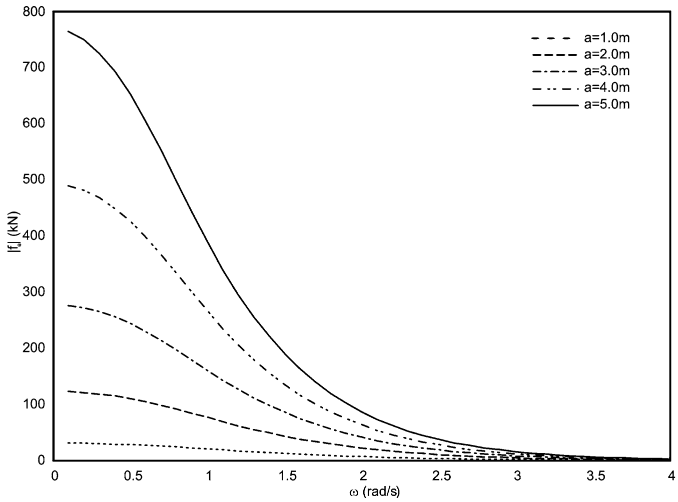

Fig. 2. The absolute value of the exciting force for heave motion versus angular frequency ω, for a vertical cylinder with different radii (a) and with a draft $b = 1.5$ m in water of depth $h = 23$ m.

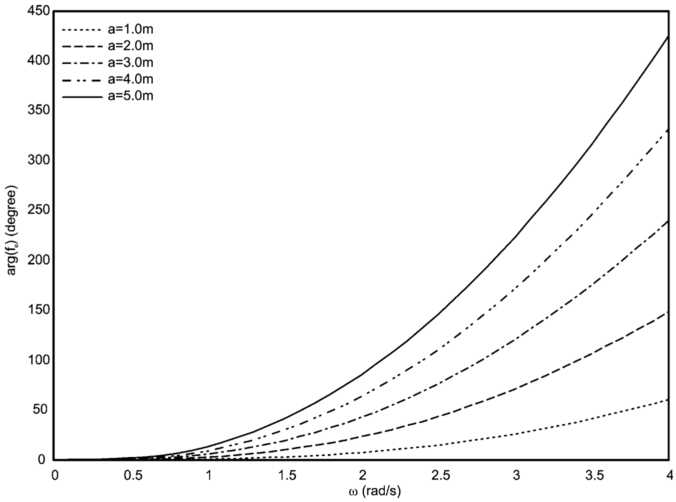

Fig. 3. The argument of the exciting force for heave motion versus angular frequency ω, for a vertical cylinder with different radii.

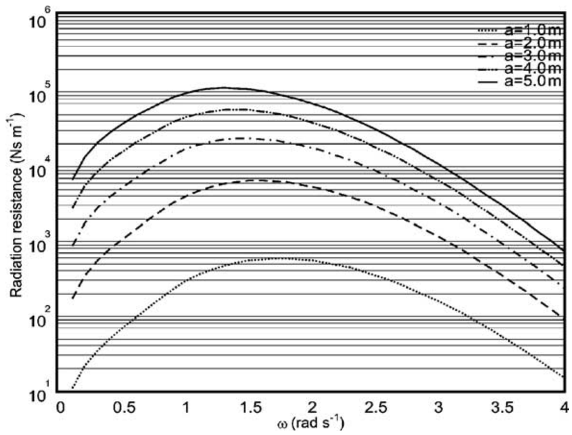

Fig. 4. Radiation resistance (R) for a circular cylinder. Same parameters as in Figs. 2 and 3.

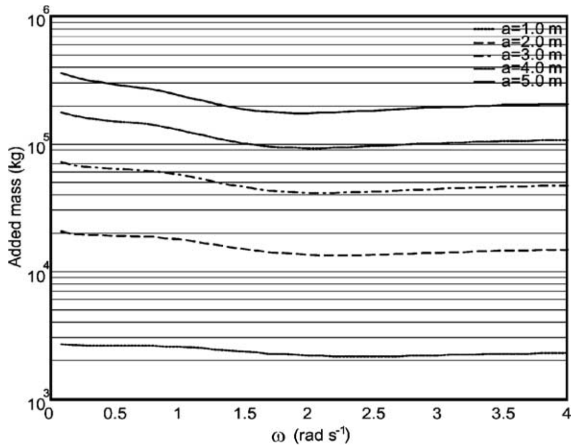

Fig. 5. Added mass (m_a) for a circular cylinder. Same parameters as in Figs. 2 and 3.

with

$$\widehat{H}(\omega) = \frac{\hat{f}_e}{-\omega^2(m_a + m) + i\omega(\gamma + R) + \rho g \pi a^2 + k_s}. \tag{11}$$

Here $\widehat{H}$ is the transfer function from the wave amplitude $\widehat{G}$ to the buoy elevation $\hat{z}$. In Figs. 6 and 7 the transfer function is plotted for different buoy radii a. The transfer function contains information about the resonance frequency, which occur when:

$$\omega = \sqrt{\frac{\rho g \pi a^2 + k_s}{m_a + m}}. \tag{12}$$

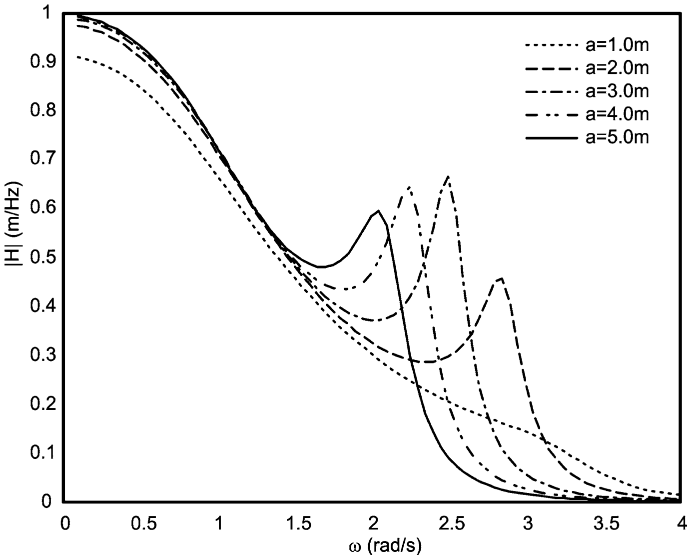

Fig. 6. The amplitude, $|\widehat{H}|$ of the transfer function $\widehat{H}$. The spring constant k_s is 3 kN/m, the damping constant γ is 3 kN s/m, the water depth is 23 m and the buoy draft 1.5 m, the total mass = 800 kg.

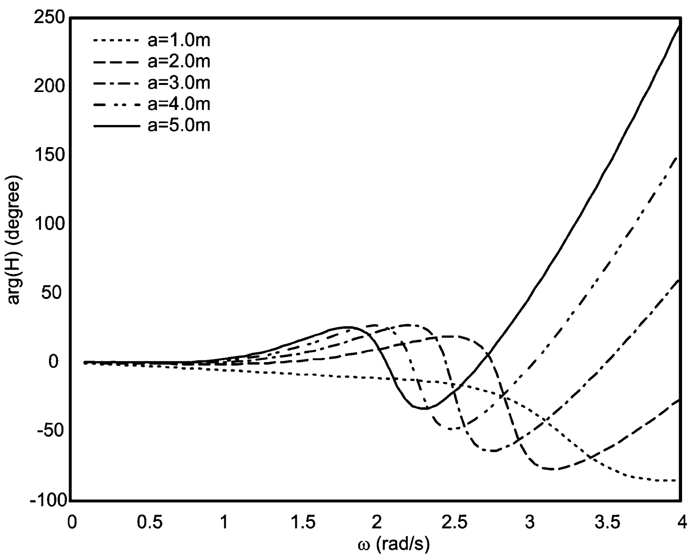

Fig. 7. The phase of the transfer function $\widehat{H}$. The same parameters as in Fig. 6.

Note that the argument of the transfer function is the sum of the excitation force phase shift and the systems phase shift. This explains why the phase in Fig. 7 is not $-90°$ when there is resonance in the system. For low frequencies the system phase shift dominates, for higher frequencies the excitation force phase shift dominates. This results in the argument of the transfer function for resonance appearing twice.

The buoy position can be computed in the time domain by taking the convolution of the wave amplitude G with the impulse response function H. The impulse response function is given by inverse Fourier transform of the transfer function $\widehat{H}$.

$$z = H(t) * G(t). \tag{13}$$

The average of the power extracted from the wave by the converter taken over the time interval $[0, t]$ is given by,

$$p(t) = \frac{1}{t}\int_0^t \gamma \dot{z}^2 \mathrm{d}t. \tag{14}$$

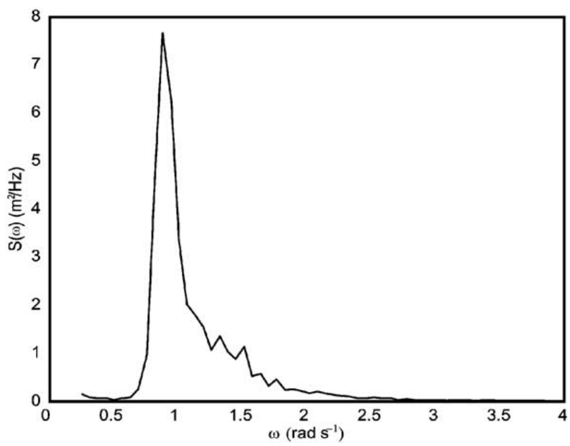

Fig. 8. Wave spectrum for wave data collected at Islandsberg, located at the Swedish west coast. Wave data collected: 2004-05-18, 10:46–11:06, significant wave height = 2.48 m.

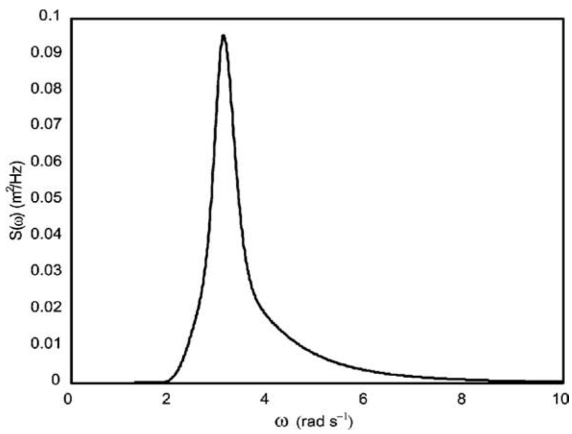

Fig. 9. A JONSWAP spectrum with peak frequency $\omega_p = 2.82$ rad/s, $\alpha = 0.185$, $\gamma = 3.3$, $\sigma_a = 0.07$ and $\sigma_b = 0.09$. The peak frequency is chosen to coincide with the resonance frequency for a buoy radius $a = 2$ m.

2.2. Waves

Two different incoming waves have been used in the simulations. The spectra are shown in Figs. 8 and 9. The spectrum in Fig. 8 is real ocean data collected at the west coast of Sweden, with a sampling rate of 2.56 Hz. The spectrum in Fig. 9 is a JONSWAP [12,13] spectrum. The parameters for this spectrum have been chosen to give a peak frequency coinciding with the resonance frequency for a system with a realistic size, in this case a buoy radius of 2.0 m.

3. Results

For an incident harmonic wave the power capture ratio increases dramatically when the natural frequency of the converter coincides with the wave frequency (see Fig. 10). The power capture ratio is here defined as the quotient of extracted power divided by the power incident on the cross section of the buoy.

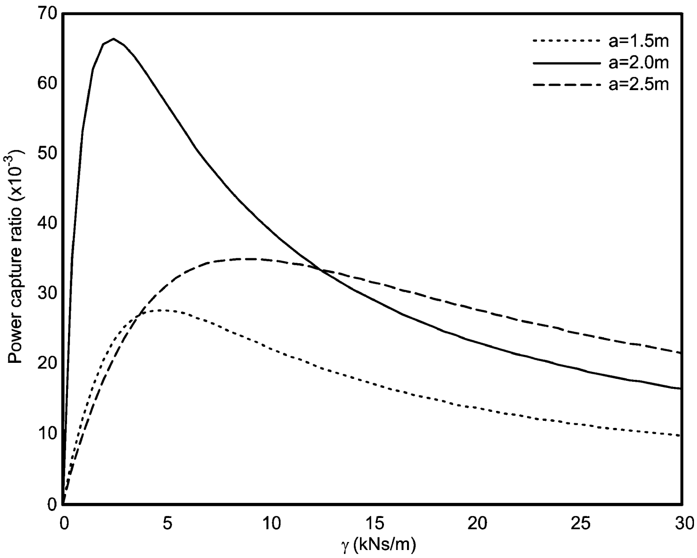

Fig. 10. Power capture ratio versus damping γ, for sinusoidal waves with different buoy radii. The wave amplitude $A = 1.0$ m, and with a buoy draft $b = 1.5$ at a water depth $h = 23$ m, the incident wave has $\omega = 2.82$ rad/s.

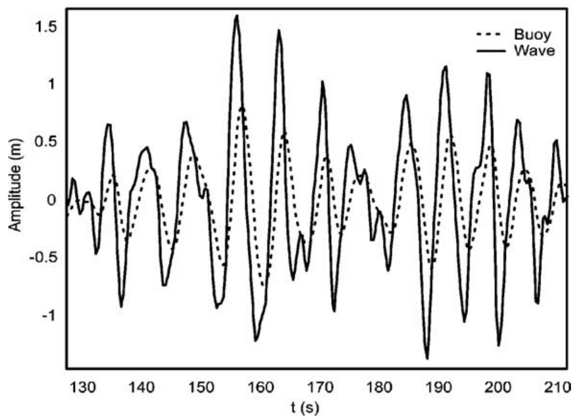

Fig. 11. Wave elevation and buoy position for an interval of wave. $k_s = 3$ kN/m, $\gamma = 30$ kN s/m, $a = 1.0$ m. Wave climate from Fig. 8.

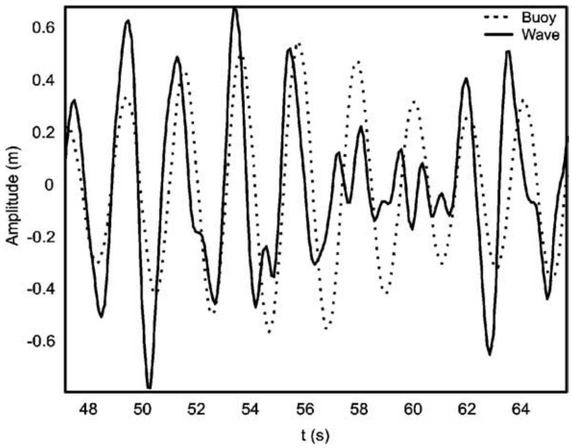

Fig. 12. Wave elevation and buoy position for an interval of wave. $k_s = 3$ kN/m, $\gamma = 4$ kN s/m, $a = 2.0$ m. Wave climate from Fig. 9.

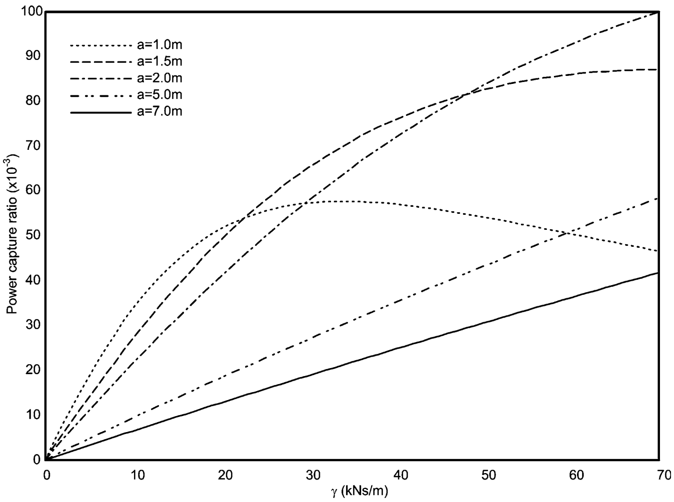

Fig. 13. Power capture ratio versus damping γ, for different buoy diameters in wave climate (8).

Fig. 11 shows the calculated response of the buoy for measured wave data. While Fig. 12 shows the response for a wave with the JONSWAP spectrum. In the first figure where the generator damping coefficient is high, this results in a buoy motion which has lower amplitude than the wave. In the second figure the dominant wave frequency coincides with the resonance frequency of the system, giving rise to large amplitudes. Note the phase difference between the incoming wave and buoy in the resonant case.

The calculated capture ratio for different buoy radii and generator damping factors are shown in Figs. 13 and 14 for the two respective wave climates. Note that the peak in power capture ratio is much more pronounced for harmonic waves (Fig. 10) than for more realistic waves (Figs. 13 and 14). This is due to the rather broad distribution of frequencies in ocean waves.

4. Discussion

For a harmonic wave, the capture ratio increases when the system is in resonance with the wave (see Fig. 10). For the case with real ocean waves, i.e. with a broader spectrum, the advantage of resonance is much

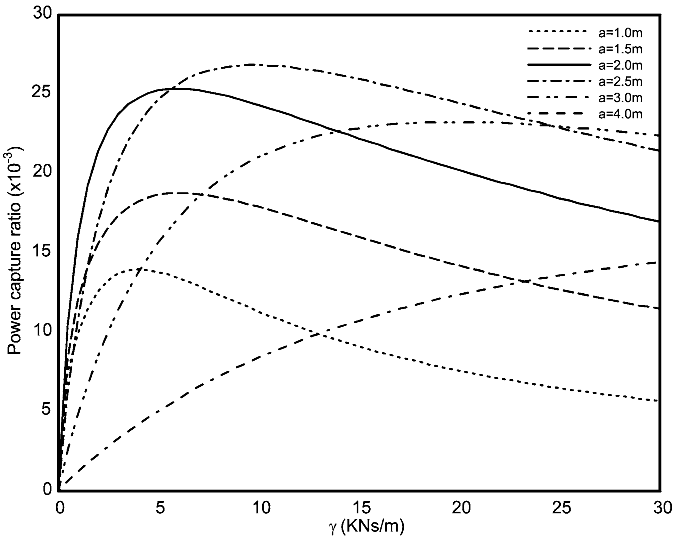

Fig. 14. Power capture ratio versus damping γ, for different buoy diameters in JONSWAP spectrum (9).

less obvious as exemplified above. The same conclusion holds in all cases we have examined. This behavior has also been observed in [18].

The natural frequency of the converter depends on the spring constant, added mass, mass, and the buoy radius (see Eq. (12)). The dominating parameters for the resonant frequency are the added mass and the buoy radius. It will therefore be difficult to shift the natural frequency of the system by changing the spring constant and the mass. This makes it hard to obtain resonance in a varying wave climate. Furthermore, to obtain resonance in a real ocean wave climate the buoy has to have a very large diameter.

When the point absorber is in resonance with the wave, the amplitude of the point absorber tends to be large. This concept does not allow large amplitudes of the alternator stroke since too large amplitudes may damage the generator structure.

This investigation is made with a generator modelled as a viscous damper. In a more thorough treatment the non-linear characteristics of the generator should be included. It is also possible to adjust the power extraction of the generator using latching or by use of power electronics. This will probably imply a different behavior of the system, and will be studied with this investigation as a starting point.

5. Conclusions

The simulations with the generator modelled as a viscous damper show that the advantage with a system in resonance with the waves is not so obvious for real ocean waves due to the broader wave spectrum. This study has not focused on optimizing the power uptake, hence power capture ratios are quite low. The resonant frequency of the converter can almost only be shifted by changing the buoy radius. This makes it difficult to use resonance in the proposed concept. Furthermore, with realistic parameters of the buoy and spring the resonance frequency of the converter is much higher than the peak frequency of real ocean waves. We have shown that it will be necessary to control the generator damping in order to obtain good power capture ratio when the wave climate changes. In the end it will be the economy of the device which decides its design.

Acknowledgements

We gratefully acknowledge our project sponsors, viz. the Swedish Energy Agency, the Ångpanneföreningen Research Foundation, the J. Gust Richert Foundation, the Vargön Alloys Foundation, the Göteborg Energi Research Foundation, the CF Environmental Foundation, and Vinnova Draka Kabel AB.

References

[1] N.J. Baker, M.A. Mueller, Direct drive wave energy converters, Reviews in Energy Renewable: Power Engineering (2001) 1–7.
[2] M.A. Mueller, N.J. Baker, A low speed reciprocating permanent magnet generator for direct drive wave energy converters, IEE Power Electronics, Machines and Drives, 16–18 April 2002, pp. 468–473.
[3] I. Boldea, S.A. Nasar, Linear electric actuators and generators, IEEE Transaction on Energy Conversion 14 (3) (1999) 712–717.
[4] E. Spooner, M.A. Mueller, Comparative study of linear generators and hydraulic systems for wave energy conversion, University of Durham, School of engineering, 2001, ETSU Report V/06/00189/REP.
[5] M. Leijon, H. Bernhoff, O. Agren, J. Isberg, J. Sundberg, M. Berg, K.E. Karlsson, A. Wolfbrandt, Multiphysics simulation of wave energy to electric energy conversion by permanent magnet linear generator, IEEE Transactions on Energy Conversion 20 (1) (2005) 219–224.
[6] M. Leijon, H. Bernhoff, M. Berg, O. Ågren, Economical considerations of renewable electric energy production—especially development of wave energy, Renewable Energy 28 (8) (2003) 1201–1209.
[7] D.D. Bhatta, M. Rahman, On scattering and radiation problem for a cylinder in water of finite depth, International Journal of Engineering Science 41 (2003) 931–967.
[8] J. Miles, F. Gilbert, Scattering of gravity waves by a circular dock, Journal of Fluid Mechanics 34 (4) (1968) 783–793.
[9] C.J.R. Garret, Wave force on a circular dock, Journal of Fluid Mechanics 46 (1) (1971) 129–139.
[10] Ronald W. Yeung, Added mass and damping for a vertical cylinder in finite-depth waters, Applied Ocean Research 3 (3) (1981) 119–133.
[11] T. Sabuncu, Hydrodynamic coefficient for vertical circular cylinders at finite depth, Ocean Engineering 8 (1981) 25–63.
[12] K. Hasselman et al., Measurement of wind-wave growth and swell decay during the Joint North Sea Wave Project (JONSWAP), Deutschen Hydrographischen Zeitschrift, Erganzungscheft 13 (A) (1973).
[13] K. Hasselman et al., A parametric wave prediction model, Journal of Physical Oceanography 6 (1976) 200.
[14] O. Danielsson, K. Thorburn, E. Sjöstedt, M. Leijon, Simulated response of a linear generator wave energy converter, ISOPE-2004, Toulon, France, 23–28 May, 2004.
[15] J. Falnes, Ocean Waves and Oscillating Systems, Cambridge university press, 2002, ISBN 0 521 78211 2.
[16] Bi-jun Wu, Yong-hong Zheng, Ya-ge You, Xiao-yan Sun, Yong Chen, On diffraction and radiation problem for a cylinder over a caisson in water of finite depth, International Journal of Engineering Science 42 (2004) 1193–1213.
[17] Y. Drobyshevski, Hydrodynamic coefficient of a floating, truncated vertical cylinder in shallow water, Ocean Engineering 31 (2004) 269–304.
[18] K. Budal, J. Falnes, Optimum operation of improved wave-power converter, Marine Science Communications 3 (1977) 133–150.